Modulation of metabolic brain networks after subthalamic gene therapy for Parkinson's disease

Andrew Feigin*†, Michael G. Kaplitt‡, Chengke Tang*, Tanya Lin*§, Paul Mattis*†, Vijay Dhawan*†, Matthew J. During¶, and David Eidelberg*†‖

*Center for Neurosciences, The Feinstein Institute for Medical Research, North Shore–Long Island Jewish Health System, 350 Community Drive, Manhasset, NY 11030; †Departments of Neurology and Medicine, New York University School of Medicine, 550 First Avenue, New York, NY 10016; ‡Department of Neurological Surgery, Weill Medical College of Cornell University, 525 East 68th Street, New York, NY 10021; §Albert Einstein College of Medicine, 1300 Morris Park Avenue, Bronx, NY 10461; and ¶Department of Molecular Virology, Immunology, and Medical Genetics, Ohio State University, Columbus, OH 43210

Edited by Marcus E. Raichle, Washington University School of Medicine, St. Louis, MO, and approved October 18, 2007 (received for review June 26, 2007)

Parkinson's disease (PD) is characterized by elevated expression of an abnormal metabolic brain network that is reduced by clinically effective treatment. We used fluorodeoxyglucose (FDG) positron emission tomography (PET) to determine the basis for motor improvement in 12 PD patients receiving unilateral subthalamic nucleus (STN) infusion of an adenoassociated virus vector expressing glutamic acid decarboxylase (AAV-GAD). After gene therapy, we observed significant reductions in thalamic metabolism on the operated side as well as concurrent metabolic increases in ipsilateral motor and premotor cortical regions. Abnormal elevations in the activity of metabolic networks associated with motor and cognitive functioning in PD patients were evident at baseline. The activity of the motor-related network declined after surgery and persisted at 1 year. These network changes correlated with improved clinical disability ratings. By contrast, the activity of the cognition-related network did not change after gene transfer. This suggests that modulation of abnormal network activity underlies the clinical outcome observed after unilateral STN AAV-GAD gene therapy. Network biomarkers may be used as physiological assays in early-phase trials of experimental therapies for PD and other neurodegenerative disease.

brain metabolism | positron emission tomography

Parkinson's disease (PD) is characterized by a progressive loss of dopaminergic neurons in the substantia nigra, which leads to abnormal functioning of interacting inhibitory GABAergic and excitatory glutamatergic pathways in components of neural networks controlling movement (1). The activity of the subthalamic nucleus (STN) is increased in PD, largely because of reduced tone of GABAergic afferent fibers from the external globus pallidus (GPe) (2). In turn, the hyperactive glutamatergic efferents drive the internal segment of the globus pallidus (GPi) and the substantia nigra pars reticulata (SNr), resulting in the alterations in thalamic and motor cortical neural activity. Based on the notion that reducing glutamatergic neurotransmission may reverse the motor deficits of PD by normalizing brain activity within these circuits, we used adenoassociated virus (AAV) to deliver the glutamic acid decarboxylase (*GAD*) gene directly into STN (3). Preclinical studies using animal models of PD suggest that transfer of the *GAD* gene into the STN can alter its activity while also increasing the evoked release of GABA in downstream targets (3–5). However, these effects cannot be directly assessed in human subjects receiving this form of gene therapy for parkinsonism.

Metabolic brain imaging with [^{18}F]fluorodeoxyglucose (FDG) and positron emission tomography (PET) can provide a means of quantifying changes in spatially distributed neural systems after antiparkinsonian therapy (6, 7). The motor manifestations of PD are associated with increased expression of an abnormal disease-related covariance pattern (PDRP) characterized by increases in pallidothalamic metabolic activity with relative reductions in premotor and parietal association regions (8, 9). Substantial evidence exists to show that pathological PDRP expression is reduced by therapeutic lesioning or deep brain stimulation (DBS) of the motor portions of GPi and STN and that these network changes correlate with clinical outcome after treatment (6, 7, 10–12). In contrast to the PDRP, these interventions do not affect the activity of the PD-related cognitive pattern (PDCP), a distinct prefrontal-parietal metabolic network associated with memory and executive functioning in nondemented PD patients (13, 14). The quantification of treatment-mediated changes in the activity of these metabolic networks may provide an objective means of gauging the effects of experimental antiparkinsonian therapy (15).

We have recently reported clinical findings from 12 patients who received unilateral STN AAV-GAD gene therapy for advanced PD (16). In the current study, we used FDG PET to assess the changes in regional metabolism and network activity that occurred with treatment. In addition to detecting localized metabolic changes in the thalamus and cortical motor regions ipsilateral to gene therapy, we found evidence of significant modulation of PDRP network activity that correlated with motor benefit. By contrast, there was no change in PDCP activity after STN gene therapy, consistent with the observed preservation of cognitive functioning in these patients. These data support a biological basis for the observed treatment response in patients undergoing this antiparkinsonian intervention.

Results

Changes in Regional Glucose Metabolism After Surgery. Regions in which glucose metabolism changed significantly after surgery are presented in Table 1 and Fig. 1. After surgery, metabolic activity changed in the thalamus and motor cortex of the operated hemisphere ($F_{2,22} = 10.84$, $P < 0.001$; one-way repeated-measures (RM)ANOVA for each of the two regions). In the thalamus (Fig. 1*A Upper*), significant metabolic reductions were present at 6 months ($P < 0.001$) and 12 months ($P < 0.005$) after surgery (Fig. 1*B Upper*). This treatment-mediated change was most pronounced in the ventroanterior (VA) and ventrolateral (VL) nuclei and in the mediodorsal (MD) nuclei. Additionally, an increase in glucose metabolism after surgery was detected in the ipsilateral primary motor area extending into the adjacent premotor cortex (Fig. 1*A Lower*). In this region, significant

Author contributions: A.F. and M.G.K. contributed equally to this work; A.F., M.G.K., M.J.D., and D.E. designed research; A.F., M.G.K., P.M., V.D., and D.E. performed research; A.F., M.G.K., C.T., T.L., P.M., and D.E. analyzed data; and A.F., M.G.K., C.T., and D.E. wrote the paper.

Conflict of interest statement: M.G.K. and M.J.D. are founders of and consultants to Neurologix, Inc., which funded the current study. Either they or their families have significant ownership interest in the company. None of the remaining authors has involvement in Neurologix, and there are no other conflicts of interest.

This article is a PNAS Direct Submission.

‖To whom correspondence should be addressed. E-mail: david1@nshs.edu.

Table 1. Regions with significant changes in glucose metabolism after gene therapy

Regions	Coordinates§			Z_{max}	Regional glucose metabolism (normalized)			
	x	*y*	*z*		Hemisphere	Baseline	6 Months	12 Months
Decreasing metabolism								
Thalamus (VL/MD)	−4	−8	6	4.16†	OP	0.927 ± 0.030¶	0.894 ± 0.028***	0.900 ± 0.033**
					UNOP	0.886 ± 0.033	0.876 ± 0.033	0.875 ± 0.036
Increasing metabolism								
Paracentral gyrus (BA 4/6)	−46	−8	20	4.53‡	OP	0.866 ±0.013	0.891 ± 0.013*	0.907 ± 0.014***
					UNOP	0.845 ±0.011	0.853 ± 0.014	0.867 ± 0.016

VL, ventrolateral nucleus; MD, mediodorsal nuclei; BA, Brodmann area; OP, operated; UNOP, unoperated. *, $P < 0.05$; **, $P < 0.005$; ***, $P < 0.001$; compared with baseline values (Bonferroni tests). †, $P < 0.05$; ‡, $P < 0.001$; corrected for multiple comparisons.
§Montreal Neurological Institute (MNI) standard space.
¶Mean ± standard error.

metabolic increases relative to baseline were present at 6 months ($P < 0.04$) and 12 months ($P < 0.0005$) after surgery (Fig. 1*B Lower*). For both the ipsilateral thalamus and motor region, changes between 6 and 12 months were not significant ($P > 0.23$), nor were the changes after surgery significant in the homologous regions of the untreated hemisphere. Operative changes in metabolic rate were also not significant ($P > 0.58$, one-way RMANOVA) for the whole brain or for each of the two hemispheres.

Network Modulation After Surgery. At baseline, the activity of the PDRP network (Fig. 2*A*) was elevated in the gene therapy groups relative to age-matched healthy control subjects ($P < 0.004$; Student's *t* test). The time course of PDRP activity after gene therapy was different for the treated and untreated hemispheres

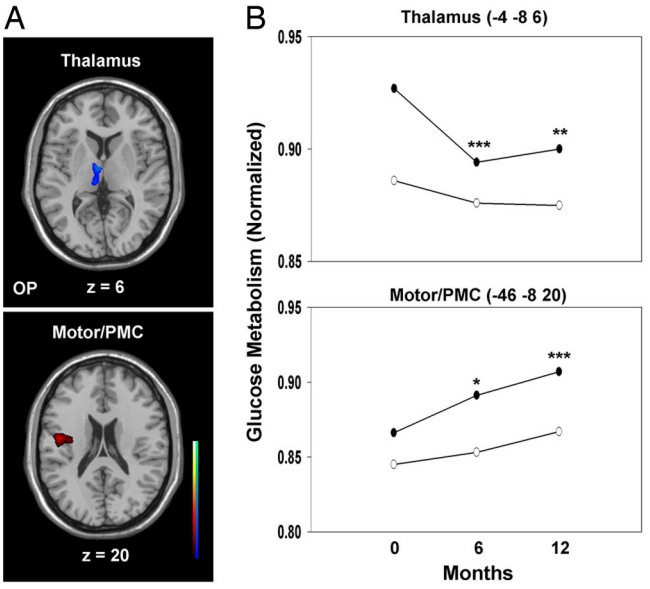

Fig. 1. Changes in regional metabolism after gene therapy. (*A*) Voxel-based analysis of changes in regional metabolic activity after unilateral STN AAV-GAD gene therapy for advanced PD. After unilateral gene therapy, a significant reduction in metabolism (*Upper*) was found in the operated thalamus, involving the ventrolateral and mediodorsal nuclei. The analysis also revealed a significant metabolic increase (*Lower*) after surgery in the ipsilateral primary motor region (BA 4), which extended into the adjacent lateral premotor cortex (PMC; BA 6). Representative axial T1-weighted MRI with merged FDG PET slices; the operated (OP) side is signified on the left. Metabolic increases after surgery are displayed by using a red–yellow scale. Metabolic declines are displayed by using a blue–purple scale. The displays were thresholded at $P < 0.05$, corrected for multiple comparisons. (*B*) Displays of the metabolic data for these regions at each time point. [In both regions, metabolic values (Table 1) exhibited significant changes over time. (*Upper*) Decreases for the thalamus. (*Lower*) Increases for the motor/PMC areas; $P < 0.001$; RMANOVA).] These regional changes were present on the operated side (filled circles) but not in homologous regions of the unoperated side (open circles). *, $P < 0.05$; **, $P < 0.005$; ***, $P < 0.001$; Bonferroni tests relative to baseline values.

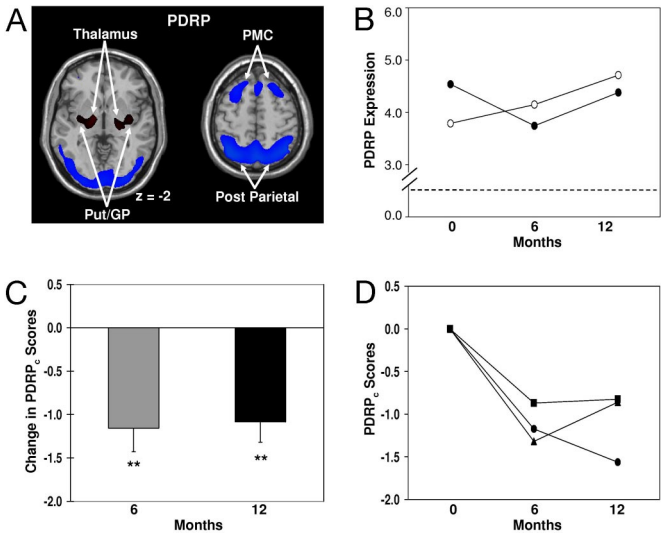

Fig. 2. Unilateral gene therapy: hemispheric changes in motor-related metabolic network activity. (*A*) PD-related metabolic pattern (PDRP). This motor-related spatial covariance pattern (9, 21) is characterized by relative pallidothalamic hypermetabolism (left) associated with relative metabolic reductions in the lateral premotor and posterior parietal areas (right). Put/GP, putamen/globus pallidus; PMC, premotor cortex. (*B*) Changes in mean PDRP network activity over time for the operated (filled circles) and the unoperated (open circles) hemispheres. After gene therapy, there was a significant difference ($P < 0.002$) in the time course of PDRP activity across the two hemispheres. In the unoperated hemisphere, network activity increased continuously over the 12 months after surgery. By contrast, in the operated hemisphere, a decline in network activity was evident during the first 6 months. Over the subsequent 6 months, network activity on this side increased in parallel with analogous values on the unoperated side. The dashed line represents one standard error above the normal mean value of zero. (*C*) Postoperative changes in PDRP activity controlling for the effect of disease progression. These progression-corrected values ($PDRP_c$ scores) reflect the net effect of STN AAV-GAD on network expression for each subject and time point (see *Materials and Methods*). Relative to baseline, $PDRP_c$ scores declined after gene therapy ($P < 0.001$, RMANOVA), with significant reductions relative to baseline at both 6 (gray bar) and 12 (black bar) months. These changes correlated ($P < 0.03$) with clinical outcome over the course of the study. **, $P < 0.005$; Bonferroni tests; bars represent standard error. (*D*) The time course of $PDRP_c$ scores according to viral vector dose. A continuous decline in network values was observed in patients receiving high-dose therapy (1×10^{12} viral genomes (vg) per milliliter (circles) but not in those receiving low (1×10^{11} vg per milliliter) (squares) or medium (3×10^{11} vg per milliliter) (triangles) doses. Four patients were treated per dose group (15). For all subjects $PDRP_c$ scores at each time point were adjusted by subtracting baseline values.

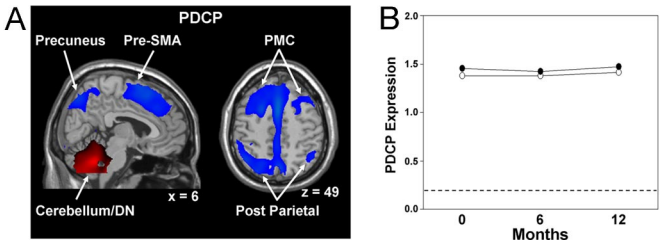

Fig. 3. Unilateral gene therapy: hemispheric changes in cognition-related metabolic network activity. (*A*) PD-related cognitive pattern (PDCP). This spatial covariance pattern (13) is characterized by relative hypometabolism in the dorsal prefrontal, premotor, and posterior parietal regions (right), associated with relative metabolic increases in the cerebellar vermis and dentate nuclei (left). pre-SMA, presupplementary motor area; PMC, premotor cortex; DN, dentate nuclei. (*B*) Changes in mean PDCP network activity over time for the operated (filled circles) and the unoperated (open circles) hemispheres. After gene therapy, there was no change in PDCP activity over time in either of the two hemispheres ($P = 0.72$). The dashed line represents one standard error above the normal mean value of zero.

(Fig. 2*B*), as indicated by the presence of a significant time × hemisphere interaction ($P < 0.002$; two-way RMANOVA). Further analysis disclosed that this interaction effect occurred in the first 6 months after surgery ($P < 0.003$). Graphical review of the time-course data revealed relatively higher PDRP expression at baseline in the clinically more affected hemisphere. After STN AAV-GAD, network activity declined on the operated side such that, by 6 months, values were lower than for the unoperated side. The trajectories of the two hemispheres increased in parallel over the subsequent 6 months.

We found that the observed time course of the network changes on the untreated side was consistent with disease progression (see *Materials and Methods*). Therefore, we used these network values to correct for disease progression on the treated side. The resulting progression-corrected PDRP scores declined significantly after gene therapy ($F_{2,22} = 10.92$, $P < 0.001$; one-way RMANOVA), with reductions relative to baseline at both 6 months ($P < 0.002$) and 12 months ($P < 0.003$) (Fig. 2*C*). These values did not change between the two postoperative time points ($P = 0.99$). Additionally, viral vector dose may have influenced the time course of PDRP modulation after gene therapy (Fig. 2*D*), although the small number of patients in each dose group precluded definitive statistical conclusions. Although there were comparable decreases in network activity from baseline to 6 months for the three dose groups (see *Materials and Methods*), a continuous decline over 12 months was observed only for the four subjects receiving the highest vector genome dose. Furthermore, for individual subjects, changes in network activity correlated with improvement in off-state Unified Parkinson's Disease Rating Scale (UPDRS) motor ratings (16) after gene therapy ($r = 0.45$, $P < 0.03$; Bland–Altman within-subject correlation).

Baseline activity of the PDCP network (Fig. 3*A*) was also elevated in the patient group relative to the controls ($P < 0.001$; Student's t test). However, there was no significant change in network activity on either hemisphere across the three time points (Fig. 3*B*; time × hemisphere interaction: $P = 0.65$, main effect of time: $P = 0.72$; two-way RMANOVA).

Comparison of Subthalamic Gene Therapy and Lesioning. To determine whether the metabolic changes associated with STN AAV-GAD were attributed to the effects of lesion rather than gene transfer, we directly compared the two interventions at key nodes of the PD network. Because clinically effective subthalamotomy is associated with prominent metabolic reductions in the thalamus and globus pallidus (11, 17), these regions were chosen for comparison with gene therapy. We found that in the treated hemispheres, operative changes in thalamic metabolism did not differ across interventions ($F_{2,15} = 0.46$, $P = 0.64$; one-way ANOVA). Metabolic activity in this region was reduced after STN surgery, whether with lesioning or AAV-GAD gene therapy (Fig. 4 *Left*). By contrast, in the treated hemispheres, changes in pallidal metabolism differed across interventions ($F_{2,15} = 9.67$, $P < 0.003$). In this region (Fig. 4 *Right*), the metabolic reductions that occurred after STN lesioning differed significantly from the changes that were observed with gene therapy ($P < 0.03$ and $P < 0.003$ for lesion versus the AAV-GAD subgroups with high and low clinical response; see *Materials and Methods*). Thus, in the treated hemispheres, declines in thalamic metabolism occurred with both STN lesioning and AAV-GAD. However, declines in pallidal metabolism occurred only with lesion, but not with gene therapy. No significant difference between interventions was evident in either of these brain regions on the unoperated hemispheres ($P > 0.28$; one-way ANOVA).

Discussion

In this functional imaging study, we observed significant metabolic changes in the thalamus and cortical motor regions of PD patients undergoing subthalamic AAV-GAD gene therapy. These regional changes occurred as part of a broadly distributed neural system that was modulated by the surgery. Indeed, these network changes measured with PET were found to correlate with concurrent assessments of clinical outcome. This information is particularly relevant in that clinical ratings were obtained by unblinded observers and are therefore potentially subject to bias. The PET results indicated that, even in this circumstance, there is objective evidence of a therapeutic response subsequent to this intervention.

A voxel-by-voxel search of the whole brain for areas in which metabolic activity changed after unilateral STN gene therapy revealed a significant treatment-mediated decline in the thalamus of the operated hemisphere, as well as a concurrent increase in ipsilateral cortical motor regions. These findings are consistent with those described after other surgical interventions for parkinsonism, including GPi and STN lesioning as well as high-frequency deep brain stimulation (DBS) of these structures (7, 10, 12, 17, 18). Nigrostriatal dopamine loss is associated with increased activity of neurons in GPi/SNr (1, 19). These, in turn, inhibit their respective targets in the VA/VL and MD thalamic nuclei (20). PD is associated with increased pallidal and thalamic glucose metabolism (10, 21), reflecting pathological increases in afferent synaptic activity in these regions (22). Indeed, levodopa therapy, which restores dopaminergic transmission in the striatum, is associated with a reduction in glucose utilization in these regions (7).

The reduction in thalamic glucose utilization after STN AAV-GAD was accompanied by concurrent metabolic increases in the lateral motor and premotor cortical regions. Similar metabolic changes have been reported after stereotaxic interventions for PD (10, 18, 23), likely caused by increases in thalamocortical activity subsequent to treatment-mediated reductions in inhibitory GPi/SNr output. The observed cortical metabolic increases are also consistent with our preclinical study in a primate model of PD (5). Overall, the metabolic changes observed after STN AAV-GAD are consistent with functional alterations within key elements of the cortico-striato-pallidothalamic-cortical (CSPTC) pathways that mediate the motor symptomatology of PD.

In addition to detecting highly localized metabolic changes after gene therapy, we also quantified changes in the activity of the PDRP, an abnormal motor-related metabolic network that is modulated by effective antiparkinsonian therapy (7, 15). By quantifying PDRP activity on a hemisphere-by-hemisphere basis (12, 17), we found that the time course of the changes on the untreated

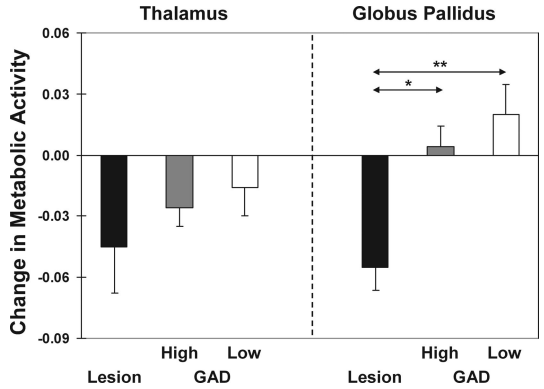

Fig. 4. Comparison of subthalamic gene therapy and lesioning. Bar graph illustrating changes in regional glucose metabolism in the thalamus (*Left*) and the globus pallidus (GP) (*Right*) after the unilateral subthalamotomy (black bar) or gene therapy (gray and white bars) for the high and low clinical response subgroups, respectively; see *Discussion*). In operated hemispheres, the declines in thalamic metabolism were not different across the three treatment groups. By contrast, reduced GP metabolism was observed only after STN lesioning but not after gene therapy. *, $P < 0.05$; **, $P < 0.005$; Bonferroni tests relative to the lesioning group; bars represent standard error.

side was consistent with the natural history of the disease (14) (see *Materials and Methods*). Computed values from this hemisphere were therefore used to control for disease progression in estimates of the net treatment effect of gene therapy on whole-brain network activity. Indeed, we found that these progression-corrected network scores declined markedly after STN AAV-GAD, with significant reductions at 6 months that were sustained at 1 year. Although the clinical assessments were performed by an unblinded rater (16), these ratings correlated with objective measures of network modulation acquired in the same subjects. This is consistent with the presence of a treatment effect distinct from, or in addition to, any disease progression that may have occurred. By contrast, unilateral STN AAV-GAD did not affect the activity of a distinct spatial covariance pattern that related to the cognitive manifestations of the disease. Like PDRP, PDCP activity was significantly elevated at baseline. However, the gene therapy had no effect on the activity of this network in either hemisphere, in accordance with the observed absence of cognitive deterioration after treatment (16).

The time course of PDRP modulation after gene therapy appeared to differ for the three dose groups. Although the declines in network scores at 6 months were similar for the three dosing tiers, continuous declines beyond this time point were observed only for the high-dose group. Although the number of subjects in each group ($n = 4$) is too small for statistical comparison, this observation points to the possibility that high-dose AAV-GAD therapy results in relatively better metabolic responses than the low and medium doses. Given that the injection volume was constant across the three dosing tiers, it is unlikely that any dose-related differences in network modulation were the result of graded subthalamic tissue injury.

It is nevertheless difficult to fully exclude an effect of damaging the STN during the gene therapy. Indeed, lesioning this structure could potentially cause clinical and imaging changes similar to those observed in our patients (17, 24). Nonetheless, in our clinical study (16), we reported no significant change in motor scores at 1 month after surgery, as would have been expected after acute STN lesioning. Moreover, significant improvement relative to the 1 month ratings was evident at later time points, suggesting that the treatment response was delayed. This is, in fact, consistent with preclinical studies suggesting that after AAV-mediated gene transfer, maximal production of the gene product is not achieved for several weeks to months (3, 5, 25, 26). These clinical observations along with an absence of radiographic evidence of STN damage at any time point, support the argument against the possibility that the observed metabolic changes were caused by lesioning.

To address this question more directly, we found that the local metabolic effects of STN AAV-GAD differed significantly from those occurring after therapeutic subthalamotomy. Reductions in thalamic metabolism occurred ipsilateral to treatment with both STN lesion and gene therapy. By contrast, pallidal reductions were present only with STN ablation, which is designed to interrupt overactive STN-GPi excitatory projections (27). The loss of this source of afferent pallidal input leads to a marked decline in GPi metabolic activity after therapeutic lesioning (17, 24). The absence of this effect after STN AAV-GAD, even in subjects with clinical benefit comparable with subthalamotomy (i.e., those in the high clinical response subgroup), likely reflects the fact that these projections are left intact after gene therapy. This is consistent with the notion that after gene therapy, the phenotype of STN neurons is altered such that GABA is now released via efferent projections to target structures, with concomitant reduction in glutamatergic outflow (3). These imaging results, combined with the time course of clinical improvement, suggest that lesioning is unlikely to explain the persistent improvement in motor function observed after gene therapy. In fact, rather than reducing pallidal metabolism, STN AAV-GAD was associated with a trend toward bilaterally increasing metabolic activity in this region. This is compatible with ongoing disease progression (14) in addition to any treatment effect that may have occurred and justifies the progression-corrected network approach that we used.

In summary, significant improvements in both regional and network-related metabolic activity were observed after unilateral STN AAV-GAD gene therapy for PD. These changes, particularly the correlation between network modulation and clinical response, are consistent with the results of other therapeutic interventions for PD. We note that a potential placebo effect cannot be ruled out in these data. Employing the imaging approach described here as part of a blinded, placebo-controlled study will help clarify the relationship between changes in metabolic activity and objective, treatment-specific efficacy outcomes.

Materials and Methods

PET. We used FDG PET to study the metabolic course of the 12 PD patients (age 58.2 ± 6.7 years) who participated in an open-label safety and tolerability study of unilateral stereotaxic infusion of STN AAV-GAD for advanced disease. The details of the AAV-GAD preparation, surgical procedures, and the clinical methods and outcomes have been presented in detail in ref. 16. Briefly, the 12 subjects had a PD duration of at least 5 years and were in Hoehn and Yahr stage 3 or more. They were divided into three equal dosing groups [low, 1×10^{11} viral genomes (vg per milliliter), medium, 3×10^{11} vg per milliliter, or high, 1×10^{12} vg per milliliter], and all received the same final injection volume of 50 μl.

All subjects were scanned off antiparkinsonian medications as described (7, 9). FDG PET scans were performed at baseline (within 1 month before surgery), with repeat imaging at 6 and 12 months after gene therapy. Ethical permission for these procedures was obtained from the institutional review boards of the participating institutions. Written consent was obtained from each subject with detailed explanation of the procedures.

Changes in Regional Metabolism After Surgery. Regional and global rates of glucose metabolism were computed on a voxel basis for each FDG PET scan as described (10). The metabolic images were processed by using SPM5 (Institute of Neurology, London) running on Matlab 6.5 (Mathworks). Images from subjects who

had AAV-GAD injected into the right STN, i.e., in whom the left limbs were more clinically affected, were reversed such that all hemispheres treated with gene therapy appeared on the left.

Changes in regional metabolism after surgery were assessed across the three time points by using the "Flexible Factorial" model in SPM. Contrasts defined as "−1 0.5 0.5" and "1 −0.5 −0.5" were used respectively to assess increasing and decreasing regional metabolism over time. Changes were considered significant at a corrected threshold of $P < 0.05$. The localization of each reported cluster was confirmed by using the Talairach space utility (www.ihb.spb.ru/~pet_lab/TSU/TSUMain.html).

For each significant cluster, we performed a post hoc analysis in which metabolic activity at each time point was measured within a spherical volume-of-interest (VOI) (radius = 4 mm) centered on the peak voxel. VOI data were also acquired around the mirror voxel in the other hemisphere. Each regional value was ratio normalized by the global metabolic rate measured in that scan. Longitudinal changes in these values were examined for each region in each hemisphere by using a one-way RMANOVA. Post hoc comparisons were performed between time points (e.g., 2-1, 3-2, 3-1) by using Bonferroni tests.

Network Modulation After Surgery. In all subjects, the activity of the motor- and cognitive-related PD spatial covariance patterns (PDRP, Fig. 2*A*; PDCP, Fig. 3*A*) were separately quantified at each time point on a hemispheric basis by using a fully automated algorithm (9, 12). These computations were performed blind to subject, hemisphere (operated, unoperated), viral vector dose (low, middle, high), time point (0, 6, or 12 months), and clinical outcome (UPDRS motor ratings). The resulting values were compared with those from 12 healthy volunteer subjects (age 55.8 ± 8.8 years).

To determine whether changes in network activity differed for the operated and unoperated hemispheres across the three time points, we performed a two-way RMANOVA for each of the two networks, which included time and hemisphere as two within-subject variables. If a significant time × hemisphere interaction effect was present on the hemispheric PDRP or PDCP network values over time, we performed two additional two-way RMANOVAs on these measures: one for the data at baseline and 6 months and the other for the data at 6 and 12 months. These piece-wise analyses allowed us to determine whether the interaction effect occurred in the first or second 6 months after gene therapy.

In analyzing the PDRP values, we observed a progressive increase in network values over time in the unoperated hemispheres of the gene therapy subjects (Fig. 5, open circles). This increase in network activity was in continuity with that observed in a group of earlier-stage PD patients (14) who underwent serial FDG PET imaging as part of a longitudinal study of disease progression (Fig. 5, open triangles). For each subject, the annual rate of change in hemispheric network activity was computed by dividing the difference between network expression at the first and third time points by the time interval. In the unoperated hemispheres of the gene therapy subjects, PDRP expression increased at a rate of 0.93 per year, which was not different from that observed in the progression study (0.64 per year; $P = 0.60$, Student's t test). To demonstrate the continuity of the two groups, we used the natural history data to calculate the predicted 95% confidence intervals for PDRP expression in the unoperated hemispheres of the gene therapy recipients at each of the three time points. We found that the observed mean values for PDRP expression in this hemisphere (3.79, 4.15, and 4.71 at baseline, 6 months and 12 months, respectively) fell within the 95% confidence intervals for values predicted based on the natural history data (baseline: 3.53–4.73; 6 months: 3.69–5.08; 12 months: 3.84–5.43).

The changes in PDRP activity on the unoperated hemispheres of the AAV-GAD patients were therefore attributed to disease progression, and for each subject and time point, these values were subtracted from those of the operated side. The resulting progression-corrected values ($PDRP_c$ scores) were used as an index of the net treatment effect of the gene therapy, i.e., the changes in network activity that remained after controlling for the effects of disease progression. Changes in the scores after treatment were examined by using a one-way RMANOVA. Post hoc comparisons were performed between time points (e.g., 2-1, 3-2, 3-1) by using Bonferroni tests. Bland–Altman within-subject correlation coefficients (28) were used to determine the relationship between changes in the $PDRP_c$ scores and motor UPDRS ratings over the three time points. Because PDCP expression did not change over time in either hemisphere (Fig. 3*B*), the progression-corrected analysis was not performed on these network values.

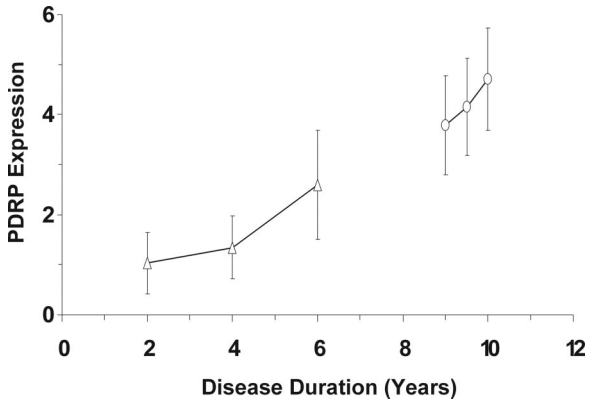

Fig. 5. Disease progression in the unoperated hemisphere. The time course of PDRP expression on the unoperated hemisphere of the AAV-GAD-treated subjects (open circles) was compared with that measured in 15 early-stage PD patients (open triangles) who underwent longitudinal FDG PET imaging over a 4-year period (13). The network values were plotted against the duration of disease at each time point. There was no difference ($P = 0.60$; Student t test) in the rate of change in network activity over time between the two groups. PDRP expression in the AAV-GAD group was observed to be in continuity with the natural history data, suggesting that the changes observed in the unoperated hemisphere were a reflection of disease progression (see *Materials and Methods*).

Comparison of Subthalamic Gene Therapy and Lesioning. Surgical ablation of the STN can give rise to clinical improvement and metabolic changes similar to those observed with subthalamic AAV-GAD (11, 17, 24). To determine whether the outcome of STN AAV-GAD was attributable to lesion rather than actual gene therapy, the effects of the two interventions on regional metabolism were compared at key nodes of the PD network. In a previous FDG PET study of six PD patients undergoing unilateral subthalamotomy for PD (17), we found that this intervention gave rise to a 58.5% reduction in contralateral limb motor off-state UPDRS ratings at 12 months. For purposes of comparison with the lesion group, the AAV-GAD recipients were divided into high and low treatment-response subgroups based on a cutoff of 40% improvement in off-state total motor UPDRS ratings at 12 months after surgery. [This cutoff was chosen based on a dichotomization of the treatment responses that was observed in the 12-month clinical data (16)]. The high-response subgroup comprised five patients with a mean change of −56.5% in contralateral limb ratings at 12 months. This cohort was therefore matched for treatment response with the lesion group. The low-response subgroup comprised seven patients with a mean change in contralateral limb scores of + 6.9% at 12 months.

Unilateral subthalamotomy is associated with significant metabolic reductions in the globus pallidus and thalamus of the operated hemisphere (11, 17). Therefore, STN AAV-GAD was compared with lesion by contrasting the changes in metabolism that occurred after treatment in these two regions. To avoid bias in the group comparisons, we used an automated, anatomically defined region-of-interest (ROI) method to quantify globally normalized metabolic activity in the globus pallidus and thalamus of the lesion group and of both AAV-GAD subgroups. This approach used a volumetric brain atlas generated from anatomical parcellation of the spatially normalized single-subject high-resolution MRI volume from the Montreal Neurological Institute (downloadable from www.fmri.wfubmc.edu/download.htm) (29, 30). These ROI computations were performed blind to treatment group (lesion, AAV-GAD), hemisphere (operated, nonoperated), and clinical response (high or low, for the AAV-GAD subgroups). For each of the two regions, we used one-way between-subjects ANOVA to compare the metabolic changes across the three groups in the operated and control hemispheres. Post hoc comparisons were performed between any two groups by using Bonferroni tests. For all analyses, the significance level was set at $P < 0.05$. Statistical analyses were performed by using SAS 9.1 (SAS Institute).

We thank Dr. Thomas Chaly for radiochemistry support, Mr. Claude Margouleff for technical support during the PET studies, and Ms. Toni Flanagan for valuable editorial assistance.

1. Wichman T, DeLong MR (2003) *Ann NY Acad Sci* 991:199–213.
2. Hamani C, Saint-Cyr JA, Fraser J, Kaplitt M, Lozano AM (2004) *Brain* 127:4–20.
3. Luo J, Kaplitt MG, Fitzsimons HL, Zuzga DS, Liu Y, Oshinsky ML, During MJ (2002) *Science* 298:425–429.
4. Lee B, Lee H, Nam YR, Oh JH, Cho YH, Chang JW (2005) *Gene Ther* 12:1215–1222.
5. Emborg ME, Carbon M, Holden JE, During MJ, Ma Y, Tang C, Moirano J, Fitzsimons H, Roitberg BZ, Tuccar E, *et al.* (2007) *J Cereb Blood Flow Metab* 27:501–509.
6. Carbon M, Edwards C, Eidelberg D (2003) *Adv Neurol* 91:175–181.
7. Asanuma K, Tang C, Ma Y, Dhawan V, Mattis P, Edwards C, Kaplitt MG, Feigin A, Eidelberg D (2006) *Brain* 129(Pt 10):2667–2678.
8. Eckert T, Tang C, Eidelberg D (2007) *Lancet Neurol* 6:926–932.
9. Ma Y, Tang C, Spetsieris PG, Dhawan V, Eidelberg D (2007) *J Cereb Blood Flow Metab* 27:597–605.
10. Fukuda M, Mentis MJ, Ma Y, Dhawan V, Antonini A, Lang AE, Lozano AM, Hammerstad J, Lyons K, Koller WC, *et al.* (2001) *Brain* 124:1601–1609.
11. Su PC, Ma Y, Fukuda M, Mentis MJ, Tseng HM, Yen RF, Liu HM, Moeller JR, Eidelberg D (2001) *Ann Neurol* 50:514–520.
12. Trošt M, Su S, Su PC, Yen R-F, Tseng H-M, Barnes A, Ma Y, Eidelberg D (2006) *NeuroImage* 31:301–307.
13. Huang C, Mattis P, Tang C, Perrine K, Carbon M, Eidelberg D (2007) *NeuroImage* 34:714–723.
14. Huang C, Tang C, Feigin A, Lesser M, Ma Y, Pourfar M, Dhawan V, Eidelberg D (2007) *Brain* 130:1834–1846.
15. Eckert T, Eidelberg D (2005) *NeuroRx* 2:361–371.
16. Kaplitt M, Feigin A, Tang C, Fitzsimons H, Mattis P, Lawlor P, Bland R, Young D, Strybing K, Eidelberg D, During MJ (2007) *Lancet* 369:2097–2105.
17. Trošt M, Su PC, Barnes A, Su SL, Yen RF, Tseng HM, Ma Y, Eidelberg D (2003) *J Neurosurg* 99:872–878.
18. Eidelberg D, Moeller JR, Ishikawa T, Dhawan V, Spetsieris P, Silbersweig D, Stern E, Woods RP, Fazzini E, Dogali M, Beric A (1996) *Ann Neurol* 39:450–459.
19. Obeso JA, Rodriguez-Oroz MC, Rodriguez M, Macias R, Alvarez L, Guridi J, Vitek J, DeLong MR (2000) *Neurology* 55:S7–S12.
20. Ilinsky IA, Kultas-Ilinsky K (2002) *Mov Disord* 17 (Suppl 3):S9–S14.
21. Eidelberg D, Moeller JR, Dhawan V, Spetsieris P, Takikawa S, Ishikawa T, Chaly T, Robeson W, Margouleff D, Przedborski S, *et al.* (1994) *J Cereb Blood Flow Metab* 14:783–801.
22. Eidelberg D, Moeller JR, Kazumata K, Antonini A, Sterio D, Dhawan V, Spetsieris P, Alterman R, Kelly PJ, Dogali M, *et al.* (1997) *Brain* 120:1315–1324.
23. Sestini S, Ramat S, Formiconi AR, Ammannati F, Sorbi S, Pupi A (2005) *J Nucl Med* 46:1444–1454.
24. Su PC, Tseng HM, Liu HM, Yen RF, Liou HH (2003) *Mov Disord* 18:531–538.
25. Herzog RW, Hagstrom JN, Kung SH, Tai SJ, Wilson JM, Fisher KJ, High KA (1997) *Proc Natl Acad Sci USA* 94:5804–5809.
26. Palomeque J, Chemaly ER, Colosi P, Wellman JA, Zhou S, Del Monte F, Hajjar RJ (2007) *Gene Ther* 14:1055.
27. Gill SS, Heywood P (1997) *Lancet* 350:1224.
28. Bland JM, Altman DG (1995) *Br Med J* 310:446.
29. Tzourio-Mazoyer N, Landeau B, Papathanassiou D, Crivello F, Etard O, Delcroix N, Mazoyer B, Joliot M (2002) *NeuroImage* 15:273–289.
30. Maldjian JA, Laurienti PJ, Kraft RA, Burdette JH (2003) *NeuroImage* 19:1233–1239.